Pharm Res (2013) 30:203–217
DOI 10.1007/s11095-012-0863-9

RESEARCH PAPER

Implementing Quality by Design in Pharmaceutical Salt Selection: A Modeling Approach to Understanding Disproportionation

Jeremy M. Merritt • Shekhar K. Viswanath • Gregory A. Stephenson

Received: 13 April 2012 / Accepted: 9 August 2012 / Published online: 24 August 2012

ABSTRACT

Purpose Salts of active pharmaceutical ingredients are often used to enhance solubility, dissolution rate, or take advantage of other improved solid-state properties. The selected form must be maintained during processing and shelf-life to ensure quality. We aimed to develop a model to quantify risk of disproportionation, where the salt dissociates back to the freebase form.

Methods A mechanistic model based on thermodynamics was built to predict disproportionation. Stress testing of molecules in combination with excipients was used to benchmark model predictions. X-ray powder diffraction and solid-state NMR were used to quantify the formation of freebase experimentally.

Results 13 pharmaceutical compounds were screened in 4 formulations containing different combinations of excipients. The test set spanned molecules which did and did not disproportionate and also formulations which did and did not induce disproportionation. Model predictions were in qualitative agreement with the experimental data, recovering trends of how disproportionation varies with humidity, formulation excipients, base pK_a and solubility of the API.

Conclusions The model can predict the balance between different driving forces for disproportionation with limited experimental data resulting in a tool to aid in early-phase risk assessment and formulation design with respect to disproportionation.

KEY WORDS disproportionation · microenvironmental pH · model · pH_{max} · quality by design

INTRODUCTION

Active pharmaceutical ingredients (API) typically fall into the category of weak electrolytes. In their neutral state, API are often poorly water-soluble, which can limit the bioavailability of the compound. Salt formation is not only used as a handle to increase solubility (1), but also to alter physical properties (hygroscopicity, melting point, polymorphism, etc.…) of the API (2). In general, strong acids are needed to form salts of basic API due to the relatively low pK_a of amine functional groups. If a salt undergoes a reaction to form the freebase as a solid-phase and the counter-ion, a disproportionation reaction is said to take place. This reaction is critically important for pharmaceutical salts in the solid-state, particularly when it impacts bioavailability or chemical stability, as it can determine the shelf life of the product (3). It is also important *in vivo* (4), as the API experiences different pH regions of the stomach and intestine en-route to absorption. Many examples of the detrimental effects of disproportionation have been reported in the literature and have been recently reviewed (5).

Electronic supplementary material The online version of this article (doi:10.1007/s11095-012-0863-9) contains supplementary material, which is available to authorized users.

J. M. Merritt · S. K. Viswanath
Chemical Product Research and Development, Eli Lilly and Company
Indianapolis, Indiana 46221, USA

J. M. Merritt (✉)
Eli Lilly & Co
DC 4816, Eli Lilly and Co., Lilly Technology Center South
1400 W. Raymond St.
Indianapolis, Indiana 46221, USA
e-mail: merrittje@lilly.com

G. A. Stephenson
Pharmaceutical Sciences Research and Development
Eli Lilly and Company
Indianapolis, Indiana 46221, USA

In addition to understanding the physical stability of the API itself, one must also understand the influence of the formulation used in the final drug product (6). Prototype formulation screens are often used to guide commercial formulation development of an oral dosage form. Accelerated stress testing of the formulation plus API at high temperature and high humidity is used to test the propensity of disproportionation and also other polymorph changes. While qualitative theories exist for interpreting experimental results of disproportionation, the goal of this work was to build a mathematical model capable of first principles prediction. Not only was the API targeted for study, but also predicting API-excipient compatibility which is crucial to understand the effects of the formulation on product stability. With such an increased understanding, better formulation design and salt selection can occur with the goal of ensuring product quality and improved patient outcomes.

MATERIALS AND METHODS

Materials

Small molecule API with 300–450 molecular weight (freebases) were considered in this study. Development samples of the API were used consisting of greater than 99% purity. API with a range of base pK_a and also solubility ratios of the salt and freebase were considered. Additionally different salts of the same API and also disalts and hemisalts were studied. Table I gives the experimental properties of the molecules studied, along with several molecules reported in the literature. Excipients were those used in our commercial manufacturing processes.

Methods

Solid-State Stressed Stability Testing

Fifty milligrams of the selected form of the pure API was combined with 120 mg of a prototypical placebo mixture and blended by hand. The compositions of formulation #1 (F1), formulation #2 (F2) and formulation #3 (F3) are detailed in Table II. These are representative formulations of what might be considered starting compositions for wet granulation, roller compaction, or capsule formulations. A binary mixture (~100 mg total) of API with sodium croscarmellose (NaCMC) was also studied in each case, as it appears to be one of the more commonly interacting excipients. A fifth sample (~100 mg) of pure API was also treated similarly, serving as a control such that changes of

Table I Experimental pK_a and Solubility Data For The Test Set of API. Note that the Equation for pH_{max} is Derived for Monosalts Only, Thus The Hemisalt and Disalt Species Do Not Have Calculated Values

Molecule	MW[A] (g/mol)	pH_{max} (calc)	pK_a (base)	pK_a (acid)[C]	S_{salt} (mol/L)	S_{FB} (mol/L)
A*HCl	419	0.68	4.8	−7	5.31E-2	5.06E-6
A*HBr	419	0.96	4.8	−8	2.78E-2	5.06E-6
A*HemiNapadisylate	419	–	4.8	−2.7, −1.9	1.31E-2	5.06E-6
Benzocaine*Mesylate (6)	165	1.29	2.8	−1.6	1.88E-1	5.80E-3
B*HCl	373	1.35	5.1	−7	9.87E-2	1.74E-5
Miconazole*Mesylate (6)	416	1.44	6.9	−1.6	6.88E-1	2.40E-6
D*HCl	303	1.53	3.2	−7	6.46E-2	1.39E-3
E*Phosphate	371	1.68	4.0	1.8	5.33E-2	8.89E-5
Benzocaine*Napsylate (6)	165	2.64	2.8	−1.8	8.36E-3	5.8E-3
F*Tosylate	445	2.73	4.9	−2.8	5.67E-4	2.25E-6
Delveridine*Mesylate (5)	456	3.53	6.8	−1.6	5.80E-1	3.13E-4
C*Maleate (26)	275	3.58	6.3	1.9 (26)	3.84E-3	7.27E-6
G*HCl	320	6.01	8.8	−7	>8.57E-1	1.37E-3
I*HCl	444	6.71	8.8	−7	8.81E-2	7.21E-4
Miconazole*Napsylate (6)	416	7.03	6.9	−1.8	1.76E-6	2.40E-6
H*Tosylate	461	8.30	8.3	−2.8	1.10E-3	1.10E-3
J*Hemisuccinate* monohydrate	517	–	10.2	4.2, 5.6	1.82E-4	<9.66E-5
K*DiHCl	438	–	7.8, 4.9	−7	>7.35E-2	2.28E-5
L*Dimesylate	422	–	6.3, 4.9	−1.6	>3.25E-1[B]	2.37E-5

[A] corresponds to freebase

[B] >200 mg/mL solubility observed at 2 h however after 24 h a hemihydrate had formed with S = 136 mg/ml

[C] MarvinSketch (version 5.2.6) prediction unless otherwise noted

Table II Placebo Composition and Saturated Solution pH of Each Excipient. Also Given are the Fitted K_{eq} Values and Simulated pH for Artificial Acid–Base Equilibria in Order to Implement the Effect of Microenvironmental pH in the Modeling of Solid-State Disproportionation

Description of Ingredients	F1 %w/w	F2 %w/w	F3 %w/w	F4 %w/w	pH	K_{eq} mol/L	pH_{sim}
Lactose Spray Dried	42.5	–	–	–	4.2	4.0E-5	4.2
Microcrystalline Cellulose PH102	42.5	43.125	–	45.0	6.9	6.0E-11	6.9
Povidone K29/32	5.0	–	–	–	3.5	1.0E-3	3.5
Croscarmellose Sodium	7.5	–	–	6.4	5–7	1.1E-5	7.5
Sodium Lauryl Sulfate	1.25	–	–	–	10.0	1.0E-10	10.0
Magnesium Stearate Vegetable EP/JP/NF	1.25	1.25	–	1	8–10	1.0E-8	9.0
Mannitol SD200	–	43.125	–	38.4	4.5	1.0E-5	4.5
Hydroxypropylcellulose HPC	–	5.0	–	3	5.9	1.6E-8	5.9
Low-Substitution HPC LH22	–	7.5	–	–	5.9	1.6E-8	5.9
Lycatab C	–	–	87.5	–	5.5	9.7E-8	5.5
Partially Pregelatinized Starch with Silicone 5%	–	–	12.5	–	5.9	1.6E-8	5.9
Solution Volume (L)[A]	7.7E-6	5.6E-6	1.2E-5	–			

[A] assumes 75% RH and 120 mg of sample

polymorphic form or states of hydration resulting from the accelerated stability conditions are distinguished from those due to microenvironment of the formulation. The samples were stored in an incubator maintained at 70°C/75% RH and removed at regular intervals for XRPD and/or solid-state NMR analysis before returning to the storage conditions.

Moisture Sorption

Moisture sorption isotherms of the prototypical formulations were recorded at 25°C and 50°C using an automated gravimetric analyzer (SGA-100, TA instruments, New Castle, DE, USA). The following experimental conditions were used: sample size approximately 20 mg, 5–95% RH adsorption/desorption range, 5% RH step interval. The minimum equilibration criterion was less than 0.01% weight gain in 15 min for a maximum time of 120 min.

Solubility

Aqueous solubilities of the salts and freebases were measured by equilibration of samples for greater than 18 h within an eppendorf shaker block equilibrated to 25°C. The supernatants were then filtered and diluted for analysis by HPLC. In several cases disproportionation of the salts was observed in the water slurry as confirmed by X-ray Powder Diffraction (XRPD) analysis of the excess solids. Solubilities were measured in these cases by determination of the solubility product (K_{sp}) by titration of excess acid until solid freebase was no longer observed. The intrinsic solubility values used in the model were calculated as the square root of the experimental K_{sp}.

pK_a

All pK_a's of Lilly compounds referred to in this work were determined experimentally by potentiometric titration.

X-ray Powder Diffraction (XRPD)

Powder diffraction patterns were collected on a X-ray powder diffractometer (D4 Endeavor, Bruker AXS, Madison, WI, USA) equipped with a CuKα source (λ=1.54056 Å) and a Vantec detector, and operated at 40 kV and 50 mA, with 0.06 mm divergence and detector slits. Each sample was scanned from 4 to 30° 2θ.

RESULTS

Experimental Results

Accelerated solid-state stability experiments (70°C/75% RH) were performed on the test set of molecules given in Table I. Each API was screened in three prototype formulations having different combinations of excipients, a binary blend with NaCMC, and also an API only control. The composition of the prototypical formulations is given in Table II and includes a range of acidic and basic excipients. The test set of API includes salts with varying stoichiometry (*i.e.* Mono, Di, and Hemi salts) and also with varying counterions (HCl, HBr, mesylate, tosylate, etc...). This dataset was used as a basis for comparing with model predictions described below.

Experimental detection of disproportionation in the solid-state stressed stability experiments was determined from XRPD or solid-state NMR analysis. Example XRPD patterns for D*HCl in F1 are given in Fig. 1. The presence

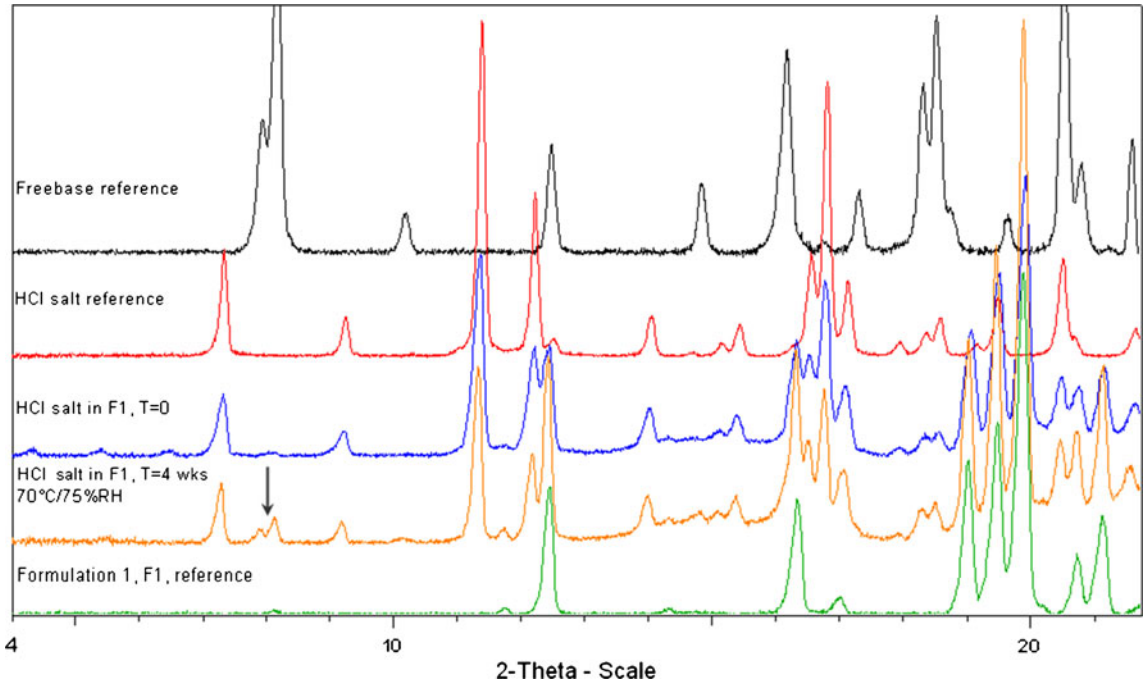

Fig. 1 XRPD comparison of D*HCl Salt in Formulation 1 stored at 70°C/75% RH for four weeks. The *arrow* indicates the peaks which are consistent with the presence of the crystalline freebase.

of crystalline freebase is detected as the appearance of the peaks indicated by the arrow. The experimental results of the stress tests for all studied molecules in the three prototypical formulations are given in Table III. Due to the early-phase of development for the molecules studied here and the rapid screening approach, a quantitative analysis method for disproportionation was not available. A qualitative + (−) is given in the table for the observation (lack of observation) of freebase after stressing for 4 weeks. The experimental limit of detection for the freebase in the placebo blend is estimated to be 5–10%. In all cases of disproportionation, the resulting XRPD patterns were in good agreement with authentic samples of crystalline freebase, illustrating that metastable freebase polymorphs were not kinetically

Table III Experimental and Model Predicted Disproportionation Results. +/− Denotes Whether Freebase was/was not Experimentally Observed

Molecule	F1 Exp.	F1 Model (%Fb)	F2 Exp.	F2 Model (%Fb)	F3 Exp.	F3 Model (%Fb)	NaCMC Binary Blend Exp.	NaCMC Binary Blend Model[B]
A*HCl	+	100.0	+	53.3	–	1.0	+	3.3
A*HBr	+	100.0	+	30.6	–	0.6	+	1.9
A*Hemi-napadisylate	–	10.3	–	1.1	–	2E-2	–	0.1
E*Phosphate	+	100.0	+	28.3	–	0.4	+	1.7
B*HCl	+	100.0	+	30.4	–	0.4	+	1.7
D*HCl	+	100.0	–	17.1	–	0.2	+	1.0
F*Tosylate	–	6.2	–	0.6	–	4E-2	–	0.1
G*HCl	–	3.2	–	0.1	–	2E-3	–	4E-3
I*HCl	–	0.1	–	3E-2	–	8E-4	–	2E-3
H*Tosylate	–	3E-3	–	2E-3	–	1E-4	–	5E-4
J*Hemisuccinate	–	7E-7	–	6E-7	–	1E-6	–	2E-5
K*DiHCl	–	6.3	–	0.1	–	3E-5	–	2E-4
L*Dimesylate[A]	–	48.2	–	3.0	–	2E-3	–	1E-2

[A] 40°C/75% RH stress conditions were employed

[B] Modeled solution volume for 50 mg NaCMC @ 75% RH=1.1E-5 L

trapped. Experimental results for the binary blends with NaCMC are also included in Table III, and in general, the extent of disproportionation was found to be similar to that observed in F1 based on the relative peak heights in the XRPD patterns. Similarly it was qualitatively observed that in all cases F2 produced less freebase than F1. No disproportionation was observed in any of the pure API control samples or in F3. The stressed stability experiments were performed at elevated temperature to increase the kinetic rate. In every instance that disproportionation was observed, the conversion appeared complete within the first 2 weeks indicating that thermodynamic equilibrium had been achieved.

All of the stressed stability experiments discussed above were performed at 75% RH. To elucidate the effect of humidity on disproportionation, existing 30°C open-dish data for B*HCl tablets was examined. The composition of the tablet formulation is given in Table II (denoted as F4). The drug load was 6.2 wt.% in this formulation. A validated XRPD method was used in this case allowing one to monitor the disproportionation quantitatively. Figure 2 shows the experimental results performed over the range of 6–33% RH. The relatively low temperature and humidity levels compared with the screening study resulted in a very slow rate of freebase formation, however, over the 2 year study equilibrium appears to have been approximately achieved. The experimental results show a relatively smooth trend of decreasing equilibrium amount of freebase with lower humidity levels. Even at time zero and the lowest humidity conditions studied, ~10% freebase was observed which was attributed to processing conditions before the material could be put on stability.

Theoretical Description of Disproportionation

Salts are chemical compounds formed by the transfer of a proton from an acid (AH) to a base (B) capable of accepting that proton. Pharmaceutical API are often weak bases and the derivations below are for this case, however the equations are easily generalized for the case of acidic API. In the solid phase, the corresponding conjugate base (A^-) and conjugate acid (BH^+) are held together by strong ionic bonds. However, when dissolved in aqueous media, the $(BH^+)(A^-)$ salt will ordinarily exist in the form of dissociated BH^+ and A^- ions. In solution one can write an equilibrium describing the ionization state as:

$$B + AH \rightleftharpoons BH^+ + A^- \tag{1}$$

where BH^+ is the protonated (API) base, B is the (API) freebase and AH and A^- are the salt forming acid and conjugate base respectively. The "salt formation" equilibrium constant for (1) as derived in detail by Brittain (7), is given by:

$$K_s = \frac{[BH^+][A^-]}{[B][AH]} \tag{2}$$

Writing out the individual equilibria and dissociation constants for the acid:

$$AH \rightleftharpoons A^- + H^+; K_a(AH) = \frac{[A^-][H^+]}{[AH]} \tag{3}$$

and base

$$BH^+ \rightleftharpoons B + H^+; K_a(BH^+) = \frac{[B][H^+]}{[BH^+]} \tag{4}$$

K_s can be simplified to:

$$K_s = \frac{K_a(AH)}{K_a(BH^+)}; pK_s = pK_a(AH) - pK_a(BH^+) \tag{5}$$

where $pK_x = -\log(K_x)$. These equations are the basis of the often cited "rule of 2" as it implies that a salt will be stabile if the ionization constants of the acid and base differ by more than 2 pK units, due to the fact that the acid–base equilibrium lies more than 100× towards the salt.

The above description of salt stability does not factor in the possibility of solids in equilibrium with the solution. Thus, in addition to the solution acid–base equilibria, the system is constrained by the maximum freebase concentration in solution (the definition of the freebase solubility, S_{FB}) and also the salt solubility S_{MS}, or more generally the solubility product K_{sp}. Water slurries are often used to test the stability of a salt with respect to disproportionation. Some of the solid salt (denoted as $MS_{(s)}$ for a monosalt: $((BH^+)(A^-)_{(s)})$) will dissolve according to the solid–liquid equilibrium and associated solubility product:

$$MS_{(s)} \rightleftharpoons BH^+ + A^-; K_{sp} = [BH^+][A^-] \tag{6}$$

If the solubility of the salt is defined as $[BH^+]$, then in the absence of excess counterion, we define the "intrinsic" salt solubility for a 1:1 (mono) salt as:

$$S_{MS} = \sqrt{K_{sp}} \tag{7}$$

As the salt dissolves, the ratio of the concentration of $[BH^+]/[B]$ and $[AH]/[A^-]$ can be calculated using their

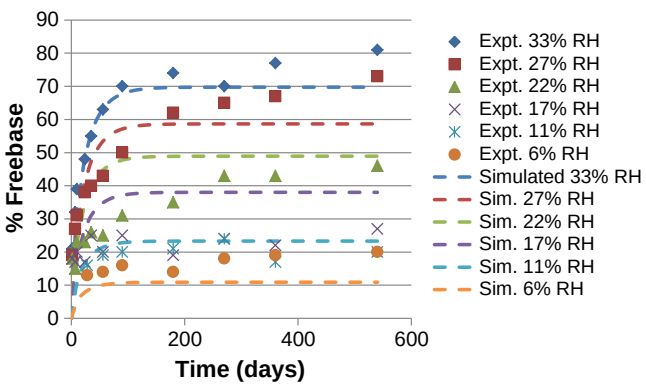

Fig. 2 Experimental and model results for B*HCl tablet disproportionation at varying levels of humidity at 30°C.

respective pK_a and also the solution pH. As the rates for acid–base reactions in solution are typically several orders of magnitude faster than the dissolution rate, the protonation equilibrium is essentially achieved instantaneously. If the concentration of the freebase exceeds its solubility, freebase will begin to precipitate, neglecting any barriers to crystal nucleation and growth. The freebase will continue to come out of solution, causing more salt to dissolve, until equilibrium is reestablished by the buildup of acid concentration. In this way it can be seen that given a very insoluble freebase, the salt may be converted to freebase in a slurry despite a favorable pK_a ratio due to a siphoning effect caused by the difference in solubilities. Because pH is dependent on the *concentration* of hydrogen ions, the amount of disproportionation (with respect to the solid phases) will depend on the initial solid loading which is an important consideration when designing experiments to test for disproportionation.

To illustrate this point further the theory proposed by Brittain can be extended by adding the solid–liquid equilibria. Note that other representations for a thermodynamic disproportionation driving force may be possible, however, only the case for when the pH=pH_{max} is considered here. At this pH, *vide infra*, the solid salt and solid freebase phases may be considered at equilibrium with one another. Consider the prototypical solution mediated solid phase disproportionation equilibrium and corresponding equilibrium constant given by:

$$MS_{(s)} \rightleftharpoons B_{(s)} + HA;\ K_{eq} = [HA] \tag{8}$$

Here the activity of the solids are assumed to be 1. The above equilibrium can be written as the sum of the four equilibria given in Table IV. The overall equilibrium constant for this disproportionation reaction is found by multiplying the individual micro-constants resulting in:

$$K_{eq} = \frac{K_a^{base}}{K_a^{acid}} * \frac{S_{MS}^2}{S_{FB}} \tag{9}$$

Thus in addition to the ratio of (K_a(base)/K_a(acid)), salt stability is shown to be related to the ratio of the solubilities. The above equilibrium was derived under the assumption of a weak acid, HA. For strong acids, there is no driving force for the acid to pair its ions and thus the prototypical disproportionation reaction involving a strong acid should be written as:

$$MS_{(s)} \rightleftharpoons B_{(s)} + H^+ + A^-;\ K_{eq} = [H^+][A^-] \tag{10}$$

The overall equilibrium constant for this disproportionation reaction will be the same as in (9) without the K_a^{acid} term. Thus once a strong acid is used, no additional salt stability should be gained by going to a stronger acid. It should be pointed out that inherent to the above derivations it is assumed that the acid (HA) is fully soluble and itself does not come out of solution.

Early-phase polymorph screens were performed for each of the Lilly salt and freebase compounds studied here and the data presented is attributed to the lowest energy crystalline form. If the freebase does not readily nucleate or crystallize in its lowest energy form, the disproportionation reaction of interest may occur to a metastable crystalline or amorphous state of the freebase. Since the solubility of amorphous and metastable crystalline states will be greater than that of the lowest energy state, the disproportionation potential would be predicted to be somewhat less.

Table IV Equilibria Describing a Prototypical Disproportionation Reaction

Equilibrium	Constants
$MS_{(s)} \rightleftharpoons BH^+ + A^-$	$K_{sp} = [BH^+][A^-] = S_{MS}{}^2$
$BH^+ \rightleftharpoons B + H^+$	K_a(base) = $[H^+][B]/[BH^+]$
$H^+ + A^- \rightleftharpoons AH$	K_a(acid) = $[H^+][A^-]/[HA]$ ($1/K_a$(acid) as written)
$B \rightleftharpoons B_{(s)}$	$K_s = [B] = S_{FB}$ ($1/K_s$ as written)

The pH of Maximum Solubility (pH_{max})

The total solubility, S_T, of an ionizable basic API will be the sum of ionized and un-ionized forms:

$$S_T = [B] + [BH^+] \tag{11}$$

In the derivation for the disproportionation equilibrium constant (9), the "intrinsic" solubilities of the freebase and salt were implied, that is, the pH was assumed to be such that only one component dictated the solubility and no common-ion effect for the salt. The pH-solubility relationship for a basic drug can be described by two independent curves, one where the freebase is the equilibrium (saturated) species and the other where the salt is in equilibrium (1,8). When the freebase is the equilibrium species, the total solubility at a given pH may be written as:

$$S_T, \text{base}(pH > pH_{max}) = S_{FB}\left(1 + 10^{pK_a^{base} - pH}\right) \tag{12}$$

The corresponding equation for when the salt is the equilibrium species is given by:

$$S_T, \text{salt}(pH < pH_{max}) = S_{MS}\left(1 + 10^{pH - pK_a^{base}}\right) \tag{13}$$

These pH dependent solubility curves are illustrated in Fig. 3, for the case of pK_a=5, S_{FB}=0.1 and S_{MS}=1. The

point at which the two curves intersect is known as pH_{max}, the pH of maximum solubility. At pH_{max}, the solid phases of the salt and freebase are in equilibrium with each other and Bogardus *et al.* derived the following expression for a base (9):

$$pH_{max} = pK_a + \log \frac{S_{FB}}{S_{MS}} \tag{14}$$

When $pH > pH_{max}$, the freebase will be the equilibrium solid phase, however when $pH < pH_{max}$, the salt will be the equilibrium solid phase. A third curve is shown in Fig. 3 illustrating the possibility of the common-ion effect on the salt solubility.

Table I contains solubility and pK_a data for some Lilly and model molecules studied here. The calculated pH_{max} values are also given in the table according to (14) and the solubility and pK_a terms of pH_{max} are also shown graphically in Fig. 4. Square (red) data points indicate disproportionation has been observed under some circumstances while triangular (blue) data points indicate no evidence for disproportionation has been observed. An imaginary boundary line has been drawn in the figure to guide the eye based on the form of the pH_{max} expression and represents a hypothetical boundary delineating disproportionation risk. Thus molecules with lower pH_{max} values (towards the lower-left quadrant in the graph) would be predicted to be at increasing risk for disproportionation. It should be pointed out however that for some of the molecules given in Table I, no disproportionation was observed for the pure solid API, but instability was induced by the formulation, or by water slurry. Thus the effects of the formulation are crucial in our understanding.

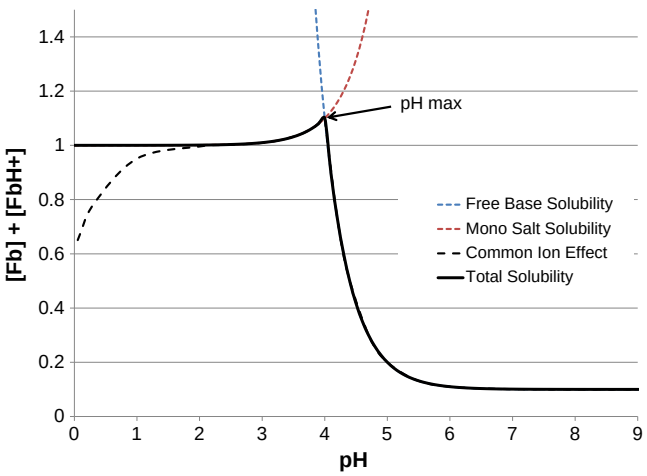

Fig. 3 Solubility–pH relationship assuming pK_a=5, S_{FB}=0.1 and S_{MS}=1. See text for details.

API-Water Slurry Model

Before tackling the influence of excipients on stability, and the leap towards understanding solid-state stability, first a model a disproportionation of just API in a water slurry was developed. Note that the model equations below are routinely used in numerical solution of chemical kinetics. The emphasis here is that with the assumption of solely a solution mediated process the disproportionation equilibrium is an exactly solvable problem. Assuming equilibrium, predictive relationships have also been published (10). The associated equilibria that were modeled in solution are given in Table V. Differential equations for all species are set up and the concentrations solved for numerically. As an example, the equation for the time dependence of the proton concentration may be written as:

$$\frac{d[H^+]}{dt} = k^f_{a_1}[HCl] - \frac{k^f_{a_1}}{K_{a_1}}[H^+][Cl^-] + k^f_{a_2}[BH^+] - \frac{k^f_{a_2}}{K_{a_2}}[H^+][B] + k^f_{a_3}[H_2O] - \frac{k^f_{a_3}}{K_w}[H^+] \times [OH^-] \tag{15}$$

where $k^f_{a_n}$ are forward rate constants and K_{a_1}, K_{a_2}, and K_w are the acid dissociation constants of the acid, protonated freebase, and water respectively. The solid–liquid equilibrium and associated rates of mass transfer of the salt and freebase were modeled according to the typical mass transport equations given by:

$$\frac{dMS_{(s)}}{dt}(mol/s) = k_L^{MS}\bar{a}\left([BH^+][A^-] - K_{sp}\right) * V_d^{MS} \tag{16}$$

and

$$\frac{dFB_{(s)}}{dt} = k_L^{FB}\bar{a}([B] - S_{FB}) * V_d^{FB} \tag{17}$$

where k_L is the mass transfer rate coefficient (m/s), ā is the specific interfacial surface area (m^2/m^3), and V_d is the dispersed (solid) phase volume. The solid densities are assumed to be 1 g/ml thus enabling the dispersed phase volumes to be calculated at a given time based on dissolution or precipitation. The initial conditions in the model include input of the weight of salt added and the initial solution volume, and assuming zero dissolved concentrations of API and pH=7 water; $[H^+]_{t=0}=[OH^-]_{t=0}$=1E-7 mol/L and $[H_2O]_{t=0}$= 55.56 mol/L. The total solution volume was imposed to be constant during the simulation. K_{sp}, S_{FB}, pK_a(AH), and pK_a (BH^+) inputs thus form the thermodynamic basis of the model. The mathematical treatment explicitly recovers the pH dependence of the API solubility

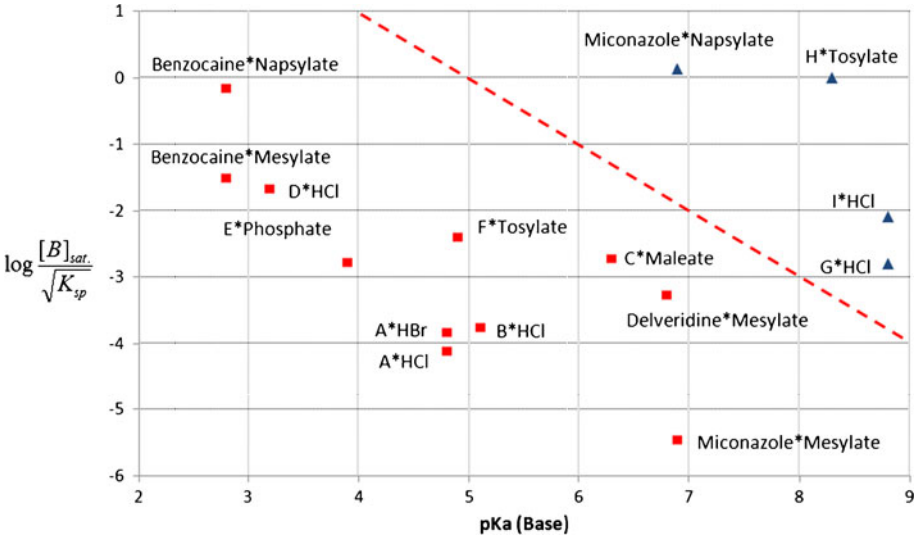

Fig. 4 Graphical plot of the terms making up the definition of pH_{max} for Lilly and model compounds. Disproportionation has been observed for the square (*red*) data points under varying conditions however no disproportionation has been observed for the data points given by the (*blue*) triangles. The dotted line is a guide for the eye based on the functional form of pH_{max} and represents a hypothetical boundary delineating disproportionation risk.

curve given the thermodynamic variables described above. The mass transfer coefficients ($k_L\bar{a}$), and solution phase rate constants $\left(k_{a_n}^f\right)$ can be treated as fitting parameters of the kinetics, however they do not influence the overall equilibrium percent freebase produced in the model. For equilibrium predictions, the coupled differential equations of the model are solved until the change in concentration of all species is zero. The reported model results are compared with the experiment by computing the percent disproportionation given by:

$$\%dispro = \frac{Freebase(mol)}{Salt^{t=0}(mol)} * 100 \tag{18}$$

The predictive capability of this approach was validated by measuring water slurry disproportionation of several API. Using experimental values for K_{sp}, S_{FB}, pK_a(AH), and pK_a (BH^+) the equilibrium amount of freebase formed under varying conditions could be predicted quantitatively. An example of this validation can be found in the Supplementary Material.

Table V Reactions in Solution Modeled for A*HCl. All Constants Reflect Room-Temperature Values

Reaction	K_{eq}
$H_2O \rightleftharpoons H^+ + OH^-$	1.8E-16 (mol/L)
$MS_{(s)} \rightleftharpoons BH^+ + Cl^-$	$K_{sp} \sim S_{MS}^2$ (mol^2/L^2)
$HCl \rightleftharpoons H^+ + Cl^-$	1E7 (mol/L)
$BH^+ \rightleftharpoons H^+ + B$	1.58E-5 (mol/L)

Model of Solid-State Disproportionation

Almost all models of solid-state reactivity rely on some mechanism for mobilization of the reagents such as by amorphous regions, defect sites, surface moisture layer, etc. Water is known to almost always play a major role at enhancing the rates (11). For crystalline solids, a model describing chemical stability in the presence of moisture is the "saturated solution layer" concept first proposed by Leeson and Mattocks in 1958 to describe the hydrolysis of aspirin (12). These concepts were also applied by Carstensen and Pothisir in developing a model of the overall decomposition rate of solid-state p-aminosalicyclic acid (13) and more recently by Guerrieri *et al.* in understanding the decomposition of procaine salts (15) and also proposed for understanding the observed shelf-life of Vitamin C (14). The model proposes microscopic "solvation" of the particles in which the some of the solid dissolves to saturation. The volume of the solution layer was expressed in terms of a moisture sorption isotherm which is a function of the relative humidity, particle surface area, and intrinsic properties of the solid. For crystalline API subject to pH-dependent degradation mechanisms, control over the microenvironmental acidity/basicity may be vital in maintaining stability as shown in a recent study that found that the degradation rates of various procaine salts in the solid state could be predicted based on solution phase (pH dependent) rate constants (15). Although deviations from the Leeson and Mattocks model have also been shown, it is a useful starting point for discussion of this work as the assumptions of the model allow one to frame the problem in an exactly solvable thermodynamic form. While there is no thermodynamic basis for "free" water in the solid-state below the deliquescence point, there is a considerable body of literature supporting surface mobility promoted by thin-film surface water

at relative humidity well below the deliquescent RH, providing evidence for a solvation mechanism (See reference (15) and references within).

In the spirit of these previous models, the solid-state disproportionation reaction was modeled by considering only the solution mediated chemistry that would occur in the surface moisture layer. Furthermore an approximation that the appropriate volume of water to be used in the model can be determined from the sum of moisture sorption isotherms of all of the solids, both API and excipients was made. This approximation is essentially the same as assuming perfect mixing of the solids, or given the relatively slow kinetics of solid-state reactions, that the diffusion time of water throughout the solids is fast such that the pH of the water layer is at equilibrium. The possibility of loss of acid either by precipitation or sublimation was also neglected at this stage. Given the high bulk water solubility of the acids used for salt formation, precipitation is not predicted in the model even given the small volumes of water at play. Sublimation, however, may be particularly important for long term storage of HCl salts due to the high volatility of HCl. Loss of acid would act to drive the equilibrium towards the freebase. At some humidity level one may expect the assumption of solely solution mediated acid–base chemistry will breakdown and thus experiments at various humidity levels will be important in understanding the limits of the proposed mechanism.

Even under relatively dry conditions, water from the atmosphere will physisorb to a crystal surface. The equilibrium amount of adsorbed water can be described by a moisture sorption isotherm, which is experimentally determined by recording the mass change as a solid is exposed to an atmosphere with controlled relative humidity. Since the amount of absorption is dependent on the surface area, this is typically normalized by considering the particle size. Although the concept of pH does not apply to solids, microenvironmental pH (micro-pH) is a term often used to represent the pH of the microscopic water layer surrounding the solid particles, in which it is assumed the solid forms a saturated solution (16). Micro-pH has been implicated as a factor influencing many solid-state reactions (17–20). Micro-pH is typically inferred from measurement of the pH of a water saturated slurry or by spectroscopically probing the ionization state of an indicator dye molecule in a solid mixture (21). Commonly used excipients and their associated micro-pH using both the saturated solution and indicator techniques have been summarized previously (5,22). Although the pH does not necessarily agree between the two measurement techniques, the general trends are typically maintained. Assuming one is interested in the stability of the salt of a weakly basic API, the basicity of some excipients may buffer the micro-pH above the salt pH_{max} resulting in disproportionation.

The effect of excipients on inducing disproportionation was taken into account in the model by assuming it is solely solution pH based. In principle, the effect of the excipients could be added to the model in the same way as the API, if defined solubility and pK_a values could be measured. Many of the excipients however are not well defined acids or bases, are often not chemically discrete, but rather exist within a range of composition, and also do not have well defined solubilities. Because the saturated solution pH can always be related to solubility and pK_a, a numerical approach to simulate the microenvironmental pH concept was adopted to model the effect of the excipients by creating a fictitious acid–base equilibrium for each excipient. An arbitrary solubility was defined (fixed at 1E-4 mol/L in the model) and the individual pK_a were fit to reproduce the experimentally observed pH of a saturated water solution for each excipient. In the model, it is assumed that the excipients are always present in an amount greater than their solubility, and there is no mutual influence on solubilities, nor a temperature dependence. An example equilibrium reaction and equilibrium constant for lactose is given by:

$$\mathrm{LactoseOH} \rightleftharpoons \mathrm{H^+} + \mathrm{LactoseO^-};$$

$$K_{eq} = \frac{[H^+][LactoseO^-]}{S_{Lactose}\left(1E-4\,\frac{mol}{L}\right)} \tag{19}$$

For excipients with acidic saturated solution pH the model is initialized with neutral solids, while for basic excipients it is initialized with anionic solids. Table II gives the fitted K_{eq} values and simulated pH for the excipients used in the prototypical formulations and their experimentally measured saturated solution pH. The acid–base equilibria associated with each excipient are added to the model along with the equilibria for the API and water and are solved simultaneously. Again kinetic parameters associated with the dissolution of the solid excipients and the solution rate constants do not impact the predictions at equilibrium.

There has been some discussion on the differences between the pH measured in saturated solutions and those measured directly in the solid-state microenvironment using an ionization probe molecule (21). While the two datasets generally correlate with each other, the magnitudes of pH are somewhat different and the ordering of individual excipients by pH is not always the same. The decision to use the solution pH to benchmark the model dovetails with the approximations already built in (solution only effects) and creates a self-consistent database. Also the solution pH is easily measured whereas only some values for excipients using the indicator dye solutions could be found in the literature. By measuring the pH and then calibrating the model to these values one may also hope to account for lot-to-lot variability or impurities in the excipients which may affect the pH. For a few excipients it was observed that the

experimental solution pH sometimes had large variability. A sensitivity analysis was performed to estimate the effects of this variability on the quality of the model predictions. For the multi-component mixtures studied here, it was determined that only the most basic excipients were important in determining the extent of disproportionation of weakly basic API.

Several values for the microenvironmental pH of Magnesium Stearate have been reported in the literature, ranging from approximately 8–10 (6,22). One hypothesis is that this pH variability is due to MgO impurities (23) which will react with water to form more soluble $Mg(OH)_2$ which is a strong base. To test this theory Mg Stearate water slurries were made up with 0.35, 3.5, and 35 mg/mL slurry density. The experimental solution pH was found to be 8.1, 9.3, and 10.3 respectively. Given that the solubility of Mg Stearate is negligible in water, the data supports the hypothesis of increased amounts of soluble impurities resulting in higher pH for higher slurry densities. Several of the excipients (povidone, hydroxypropyl cellulose, lactose, sodium lauryl sulfate, and sodium croscarmellose) did not form saturated solutions, instead forming thick gels at high loading. The reported pH of these excipients were taken as an extrapolation to high densities.

Considering the variability of some of the excipients pH and the extrapolation of saturated solution pH to microhydration environments, the definition of the "correct" pH to use in the model is somewhat subjective. Ultimately given sufficient solid-state data the individual microenvironmental pH could be viewed as fitting parameters, however there was no attempt to perform this here. The slurry pH of F1, F2, and F3 without API were determined experimentally and predicted using the model to test the method of modeling the microenvironmental pH. A minimal amount of water was added to the premixed solids, making a smooth paste, to allow all excipients to stay above their solubility. The experimental pH was 6.42, 6.35, and 5.80 compared with the model predictions of 6.44, 6.50, and 5.61 for F1, F2, and F3 respectively. The good agreement lends support to the approximations made and saturated solution pH values used.

In agreement with the model of Leeson and Mattocks, the volume of water used in the model was determined from moisture sorption isotherms. Given individual moisture sorption isotherms of each component the composite moisture sorption isotherm was calculated according to (24):

$$f_{formulation}(RH) = \sum_{i=1}^{i=n} x_i f_i(RH) \tag{20}$$

where $f_{formulation}$(RH) and f_i(RH) represent the moisture sorption isotherms of the formulation + API and the ith ingredient in the formulation respectively. x_i is the weight fraction of the i^{th} ingredient. A 6th order polynomial was used to fit each individual f_i(RH). Note that at this time a normalization of the water adsorption for the surface area of the particles has been neglected however for all experiments described here the VTI measurements were performed on the same lot of materials as those used in the experiments. The moisture sorption properties of several formulations were compared with that predicted from summing up the individual components and agreement within a factor of 2 for the water content was found. Similar agreement with other combinations of excipients has also been reported (24). Using this methodology the model is capable of predicting the composite moisture sorption curve for any combination of excipients however when experimental data for the whole formulation was available it was used. The moisture sorption isotherms for the prototypical formulations are given in Fig. 5. Based on the VTI data, the solution volumes used in the model are in the range of 5E-6 to 1E-5 L assuming 75% RH and 120 mg of formulation. The exact volumes used in the simulations of the prototypical formulations are given in Table II while that of the binary blend with NaCMC is given in Table III. The VTI moisture balance used for recording the adsorption isotherm had a upper limit of 50°C. Negligible differences were observed for the equilibrium amount of moisture adsorption for the prototypical formulations and also sodium croscarmellose from 25 to 50°C supporting the use of 25°C data in the simulation of 70°C stress experiments. The kinetics of adsorption however were increased at elevated temperature.

DISCUSSION

The first principles model results for each molecule in the three prototypical formulations is given in Table III. There were no adjustable parameters for the freebase yield. All of the model inputs came from the available experimental data. Considering the experimental limits of detection are ~5–10% freebase, the model and experimental results are in qualitative agreement for F1, F2, and F3 with the exception of the L*Dimesylate salt which the model predicts ~48% disproportionation in F1 however none was observed experimentally. It should be pointed out that molecule L was stressed at 40°C/75% RH for 4 weeks in contrast to all other molecules which were stressed at 70°C/75% RH. Given the level of agreement across the whole range of test molecules, the poorer agreement for molecule L might be attributed to a kinetic effect, and the experiments are not at the thermodynamic equilibrium. Solid-state ^{13}C NMR measurements confirmed the absence of freebase ruling out the possibility of formation of non-crystalline freebase. Additional experiments were carried out slurrying the L*Dimesylate salt in water for 24 h and a hydrated crystal

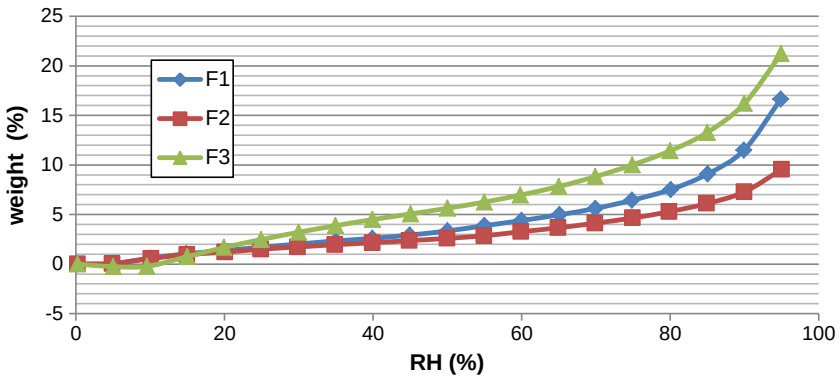

Fig. 5 Moisture sorption isotherms for the prototypical formulations.

form of the salt was observed. Form conversion to the hydrate was not observed in the solid-state stressed stability experiments however demonstrating that this polymorph is kinetically stable in the solid-state and may be important in rationalizing the lack of observed disproportionation.

Both the model and experiments show no disproportionation for any molecule in F3. This is rationalized in the model by comparing the microenvironmental pH. F3 lacks the most basic excipients found in F1 and F2, resulting in less driving force for freebase formation. While the experimental results were qualitative in nature, it was clear that when F1 and F2 induced disproportionation, F1 always produced more freebase than F2. This fact is reproduced in all of the model simulations. Based on the calculated formulation pH (F1=6.44, F2=6.50, and F3=5.61) however, this was initially puzzling. Namely more disproportionation was observed and predicted in F1, yet F2 was predicted to be slightly more basic than F1. The effect of different water volumes was ruled out as this was tested *in silico* using the model. The effect is rationalized by considering the combined formulation + API microenvironmental pH. Thus for salts of weak bases, the acidity of the API overwhelms the acidic excipients and the pH equilibrium is setup between the strong acid and the most basic excipients. F1 contains sodium lauryl sulfate which is measured to be the most basic excipient in the formulations and thus the model predicts a higher driving force for disproportionation.

Given that the experimental results showed comparable levels of disproportionation in F1 and the binary blend with NaCMC, it appears the model consistently underestimates the disproportionation potential in this case. This is rationalized by the weakly basic nature (pH ~ 5–7) observed in saturated water slurries, which the model is calibrated against. Given the weak basicity, the driving force is not predicted to be as strong as compared with other excipients. The extreme hygroscopicity of NaCMC however partially makes up for its weak basicity. In considering the possible reasons for the discrepancy of predictions for NaCMC it was realized that the current approach (defining a fixed solubility and fitted K_a to reproduce the saturated solution pH), and even the concept of microenvironmental pH, does not account for pH buffering when comparing different excipients. In the case of a buffer, the buffering strength will be crucial in addition to the final saturated solution pH. Because the current form of the model does not take into account buffering explicitly, this could increase the disproportionation potential of NaCMC considerably. To test this hypothesis buffering capacity experiments were performed for three slurry densities of NaCMC and microcrystalline cellulose PH102 (MCC) by titration with aqueous HCl. MCC was chosen as an example of an excipient with no acidic or basic functionality but giving similar saturated pH to that of NaCMC. The results of the titration experiment are given in Fig. 6 and revealed a definite effect of slurry density on buffering capacity and that NaCMC has a much larger buffer capacity than MCC for a given slurry density. While it is unclear how this behavior might scale to microhydration environments, it emphasizes that in some cases a buffering strength may be needed to rationalize the experimental results. The effect of buffering could be added to the present model by programming in buffering equilibria or by adjustment of the K_{eq} values in Table II, thus defining an effective pH. When NaCMC is formulated with a stronger base, such as in F1 and F2, this effect of buffering is not likely probed by the experiments. Clearly more in depth studies involving both binary blend data and multi-component mixtures and also buffer titration measurements of the excipients are warranted to further test this hypothesis.

Model calculations were also performed to simulate the solid-state stability studies of B*HCl in tablets at varying humidity levels given in Fig. 2. Note that the kinetic rate in the model was adjusted to match the experimental profiles however the thermodynamic limit had no adjustable parameters. The model predicts a smooth decrease in the equilibrium amount of freebase produced as the relative humidity is lowered in qualitative agreement with experiment. The water volumes used in the simulations were 2.81E-6, 2.36E-6, 1.97E-6, 1.53E-6, 9.39E-7, and 4.39E-7 L for %RH=33, 27, 22, 17, 11, and 6 respectively. It is interesting to note that the disproportionation profiles have the shape of classic first-order kinetics. When considering high levels of conversion, many solid-state degradation profiles exhibit sigmoidal shape. Such

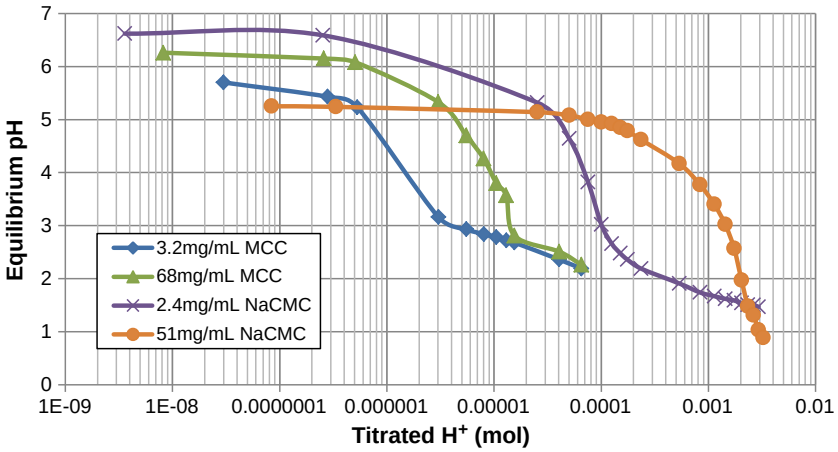

Fig. 6 HCl titration experiment to determine the buffering strength of MCC and NaCMC slurries at different slurry density. Equilibrium pH is plotted after each addition of aqueous HCl.

kinetic behavior has been rationalized by models based on the concept of nucleus branching and pharmaceutical applications invoking the Prout-Tompkins model has been reviewed (25). The difference in kinetic profiles may be supporting evidence that the observed mechanism for disproportionation could be solution mediated under this humidity range.

Sensitivity analyses were performed to assess the impact of uncertainty of the model inputs to the predictions. All of model simulations discussed thus far were performed using existing solubility data that was collected at room temperature. The solid-state stressed stability experiments were performed at 70°C thus in principle solubility data should be used to reflect these conditions. Temperature dependence of the solubility for each of the molecules studied was not available thus a sensitivity analysis was performed to assess the impact of this assumption. The temperature dependence of solubility can be calculated given the enthalpy of dissolution, which can be measured directly using calorimetry or indirectly by fitting solubility *versus* temperature data using the van't Hoff Eq. (21). Typical values for enthalpy of fusion for pharmaceutical molecules range from 50 to 100 J/g. For the sake of the sensitivity analysis, the enthalpy of dissolution is assumed to be the same as the enthalpy of fusion. Simulations at 70°C were performed for four limiting scenarios for the enthalpies of dissolution of the salt and freebase pairs, namely $\Delta H_{FB}=\Delta H_{salt}=50$ J/g, $\Delta H_{FB}=\Delta H_{salt}=100$ J/g, and $\Delta H_{FB}=50$ J/g while $\Delta H_{salt}=100$ J/g and $\Delta H_{FB}=100$ J/g while $\Delta H_{salt}=50$ J/g. The results given in Table III represent the limiting case of $\Delta H_{FB}=\Delta H_{salt}=0$ J/g. Solubility values at 70°C were thus calculated according to the van't Hoff equation:

$$ln\left(\frac{S_{70C}}{S_{25C}}\right) = -\frac{\Delta H}{R}\left(\frac{1}{343K} - \frac{1}{298K}\right) \quad (21)$$

The results of the simulations are given in Table VI. One can see that only simulations which predicted intermediate disproportionation are affected by the uncertainty. Clearly for the most quantitative comparison solubility data at the temperature of interest (or accurate enthalpies of dissolution) should be employed in the model and is an area of future interest to more accurately test the model predictions and assumptions.

Sensitivity analyses were also performed with respect to uncertainty in acid and base pK_a. Figure 7 shows a two-dimensional response surface for predicted disproportionation as a function of the two pK_a. The simulations were performed assuming 1E-5 L water and salt and freebase solubilities of 0.1 and 0.0001 mol/L respectively, and 1E-5 mol salt present at time zero. The arrows in the figure point to regions of the surface illustrating two limiting cases. In the case of a strong acid the predicted disproportionation is insensitive to the acid pK_a, even for intermediate ranges of disproportionation, while for weak acids there is a 1:1 relationship with variation of the base pK_a, *i.e.* decreasing the base pK_a by one unit has the same effect as increasing the acid pK_a by one unit and *vice versa*. Again, only for simulations with intermediate range of disproportionation would variation in base pK_a be significant. Thus uncertainties regarding the utilization of the experimentally determined base pK_a is expected to be small. This has an important implication that very early-phase estimates for risk of disproportionation could be enabled using pK_a prediction software.

An additional approximation invoked in this work is that the activity coefficients of all species are unity to simplify the calculations such that only concentrations are dealt with in the rate and equilibrium equations. Estimation of the activities, as detailed in the Supplementary Material, illustrates that the effect on the predicted percent disproportionation is likely small for the water-slurry experiments. In the modeling of the formulations, excipients could have a large contribution to the

Table VI Sensitivity Analysis of Predicted % Disproportionation Illustrating the Effect of Uncertainty on the Temperature Dependence of Solubility Data. Estimated Enthalpy of Dissolution Data of Freebase and Salt Pairs (ΔH_{FB}, ΔH_{salt} in J/g) Was Used to Predict the Temperature Dependence. See Text for Details

	ΔH_{FB}, ΔH_{salt}	ΔH_{FB}, ΔH_{salt}	ΔH_{FB}, ΔH_{salt}	ΔH_{FB}, ΔH_{salt}	ΔH_{FB}, ΔH_{salt}
	0,0	50,50	100,100	50,100	100,50
Formulation 1					
B*HCl	99.98	99.99	99.99	99.99	99.98
D*HCl	99.95	99.98	99.99	99.99	99.95
F*Tosylate	6.19	18.11	51.6	93.05	9.95
I*HCl	0.09	0.10	0.14	1.89	0.04
Formulation 2					
B*HCl	30.34	54.60	98.38	99.90	33.35
D*HCl	17.02	27.95	45.89	68.53	18.72
F*Tosylate	0.65	1.85	5.26	9.47	1.03
I*HCl	0.03	0.04	0.04	0.07	0.02
Formulation 3					
B*HCl	0.37	0.46	0.53	1.35	0.22
D*HCl	0.24	0.28	0.31	0.64	0.20
F*Tosylate	0.04	0.08	0.12	0.20	0.05
I*HCl	7.9E-04	8.6E-04	1.0E-03	1.6E-03	5.3E-04
NaCMC binary blend					
B*HCl	1.83	2.92	4.17	8.61	1.41
D*HCl	1.03	1.55	2.19	3.81	0.89
F*Tosylate	0.08	0.16	0.30	0.60	0.11
I*HCl	2.4E-03	2.6E-03	3.0E-03	4.9E-03	1.6E-03

ionic strength resulting in somewhat larger errors. The effect was still predicted to be below the experimental uncertainty reported here however. The effect of the excipients also mostly produces an absolute shift in the predictions thus the relative comparison is still valid.

Formulation/Product Design

The ability of the model to predict the effects of excipients on the solid-state microenvironmental pH, and thus disproportionation potential, either quantitatively or qualitatively

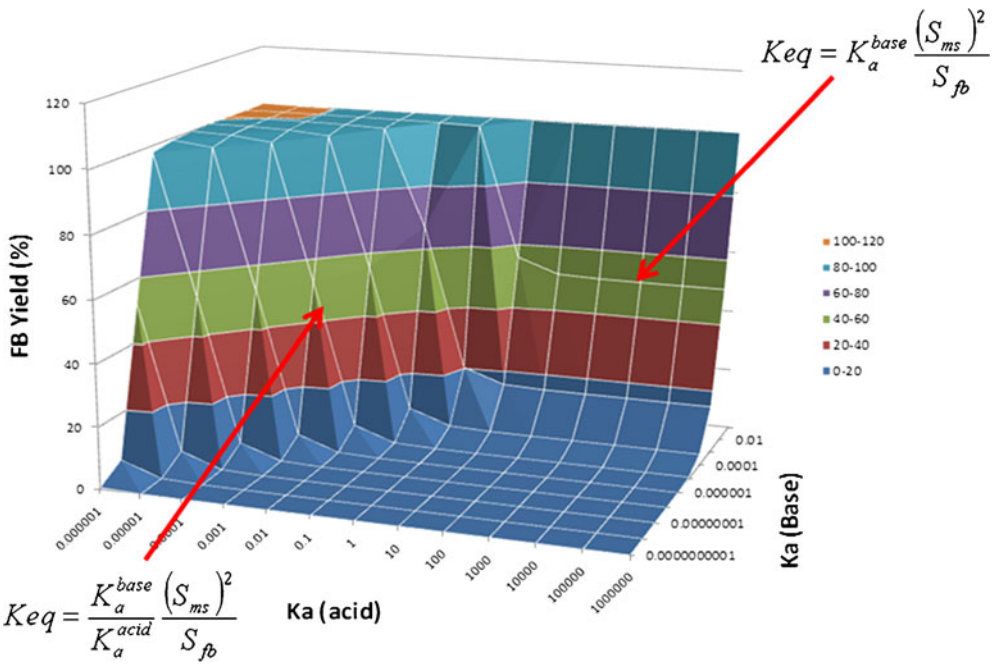

Fig. 7 Disproportionation response surface illustrating the effect of base pK_a (API) and acid pK_a (Salt former) on the percent freebase formed assuming a solution volume of 5E-6 L and salt and freebase solubilities of 0.1 and 0.0001 mol/L respectively. The arrows point to regions of the surface illustrating two limiting cases. In the case of a strong acid the predicted disproportionation is insensitive to the acid pK_a, while for weak acids there is a 1:1 relationship with the base pK_a.

in terms of trends, gives one a tool to help make informed decisions (predictions) regarding formulation design taking the API properties into account. While Fig. 2 illustrated that a viable control strategy to mitigate disproportionation in B*HCl could be focused solely on strict control of the humidity, another possibility would be to revisit the formulation to remove the basic excipients. Due to the lubricating and swelling properties of magnesium stearate and sodium croscarmellose respectively, they are widely used in pharmaceutical formulations and have been implicated as the cause of disproportionation in many cases. If due to manufacturability concerns, problematic excipients (with respect to pH) cannot be removed or substituted from the formulation, another possibility exists to add acidic or basic pH modifiers to the formulation. Serajuddin *et al.* have reported on the stabilization of the maleate salt of a basic drug by adjustment of the microenvironmental pH in solid dosage form using citric acid (26). Again, the model presented here can be used to scope out this possibly and provide a starting point for variables such as acid strength and loading. As a proof of concept, the model was altered to include the possibility of adding solid acids to the formulation. Predictions were made for the effect of solid citric and para-toluene sulfonic acid (pTSA) on the disproportionation of D*HCl in the prototypical formulation 1. The model predicted a slight decrease in % freebase for citric acid however the much stronger pTSA was predicted to stop the disproportionation completely. Stressed stability experiments were initiated to investigate if the acid could indeed inhibit disproportionation. 5 wt.% pTSA monohydrate was added to the F1 formulation and both a neat sample and one containing pTSA were stored at 70°C/75% RH and stressed for 5 weeks. Figure 8 shows XRPD scans for the initial and 5 week time points. The peak at ~8° 2θ is a good indicator of crystalline freebase. One can clearly see that the addition of the acid has inhibited disproportionation in agreement with the model predictions. The results also support the assumption of good mixing of the solids, as incomplete suppression of disproportionation might be expected for such a small acid loading given poor blending/mobility of the micro-hydration environment.

CONCLUSIONS

A method to numerically predict salt-disproportionation including the effects of excipients has been presented. Key to the model predictions is how the excipients saturated solution pH is utilized to describe the microenvironmental pH. The model framework allows the thermodynamic equilibrium of disproportionation to be determined without any empirical parameters. Thus given salt and freebase aqueous solubility and pK_a data one could make an immediate prediction of the stability of the salt with respect to disproportionation. The model allows the user to virtually select any combination of excipients, thus enabling rapid prediction of incompatibility, aiding in greater understanding and formulation design to reduce the risk of disproportionation, and possibly highlighting when costly long term stability studies are appropriate. Experimental results from both water slurry and accelerated solid-state stability studies were in qualitative agreement with the model predictions, supporting the approximations made at this stage. Qualitative agreement with the multicomponent mixtures was observed however larger descrepancies were observed in the binary blend data with NaCMC. It was proposed that buffering strength in addition to final pH may be crucial in understanding the driving force. Thus additional quantitative data combining disproportion in

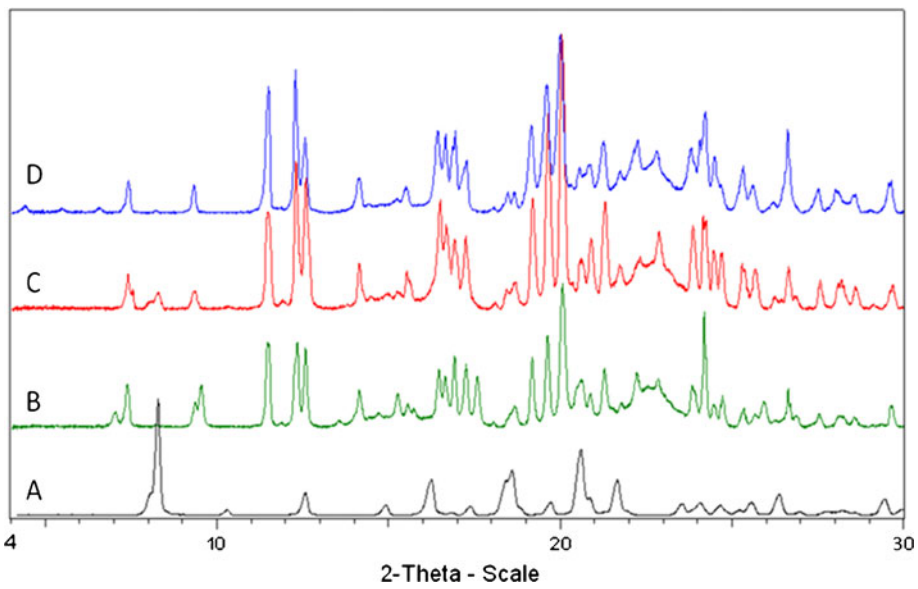

Fig. 8 XRPD traces for 5 week stress stability samples of D*HCl in Formulation 1 with and without added pTSA. (**a**) Reference pattern for the freebase. (**d**) HCl salt in formulation 1 at the start of the experiment. (**b** and **c**) 5 week time points at 70°C/75% RH with and without added pTSA respectively.

binary blends and modeling of excipient pH titration curves is needed to further test and enhance the predictions.

ACKNOWLEDGMENTS AND DISCLOSURES

Tim Woods, Adam McFarland, John Rose, Susan Reutzel-Edens, Bob Behme, and Ron Iacocca are thanked for many fruitful discussions.

REFERENCES

1. Serajuddin ATM. Salt formation to improve drug solubility. Adv Drug Del Rev. 2007;59:603–16.
2. Wermuth CG, Stahl PH editors. Handbook of pharmaceutical salts: properties selection and use. Wiley-VCH; 2002 pp 1–7.
3. Rohrs BR, Thamann TJ, Gao P, Stelzer DJ, Bergren MS, Chao RS. Tablet dissolution affected by a moisture mediated solid-state interaction between drug and disintegrant. Pharm Res. 1999;16 (12):1850–6.
4. Chen LR, Wesley JA, Bhattachar S, Ruiz B, Bahash K, Babu SR. Dissolution behavior of a poorly water soluble compound in the presence of Tween 80. Pharm Res. 2003;20(5):797–801.
5. Stephenson GA, Aburub A, Woods TA. Physical Stability of salts of weak bases in the solid-state. J Pharm Sci. 2011;100:1607–17.
6. Guerrieri P, Taylor LS. Role of salt and excipient properties on disproportionation in the solid-state. Pharm Res. 2009;26:2015–26.
7. Brittain HG. Strategy for the prediction and selection of drug substance salt forms. Pharm Technol. 2007;31:78–88.
8. Kramer SF, Flynn GL. Solubility of organic hydrochlorides. J Pharm Sci. 1972;61:1896–904.
9. Bogardus JB, Blackwood RK. Solubility of doxycycline in aqueous solution. J Pharm Sci. 1979;68:188–94.
10. Anderson BD, Conradi RA. Predictive relationships in the water solubility of salts of a nonsteroidal anti-inflammatory drug. J Pharm Sci. 1985;74:815–20.
11. Carstensen JT. Solid state stability. In: Drug stability: principles and practices. 3rd ed. New York: Marcel Dekker; 2000 pp. 166.
12. Leeson LJ, Mattocks AM. Decomposition of aspirin in the solid-state. J Am Pharm Assoc. 1958;47:329–33.
13. Carstensen JT, Pothisiri P. Decomposition of para-aminosalicyclic acid in solid-state. J Pharm Sci. 1975;64:37–44.
14. Hiatt AN, Taylor LS, Mauer LJ. Influence of simultaneous variations in temperature and relative humidity on chemical stability of two vitamin C forms and implications for shelf life models. J Agric Food Chem. 2010;58:3532–40.
15. Guerrieri P, Jarring K, Taylor LS. Impact of counter ion on the chemical stability of crystalline salts of procaine. J Pharm Sci. 2010;99:3719–30.
16. Serajuddin ATM, Jarowski CI. Effect of diffusion layer pH and solubility on the dissolution rate of pharmaceutical acids and their sodium salts. Part 2. Salicylic acid, theophylline, and benzoic acid. J Pharm Sci. 1985;74:148–54.
17. Badawy SIF, Williams RC, Gilbert D. Effect of different acids on solid-state stability of an ester prodrug of an iib/iiia glycoprotein receptor antagonist. Pharm Dev Technol. 1999;4:325–32.
18. Thakur AB, Morris K, Grosso JA, Himes K, Thottathil JK, Jerzewski RL, *et al.* Mechanism and kinetics of metal ion-mediated degradation of fosinopril sodium. Pharm Res. 1993;10:800–9.
19. Serajuddin ATM, Rosoff M. pH-solubility profile of paverine hydrochloride and its relationship to the dissolution rate of sustained-release pellets. J Pharm Sci. 1984;73:1203–8.
20. Carstensen JT, Rhodes CT. Drug stability: principles and practices. New York: Marcel Dekker; 2000. p. 199.
21. Pudipeddi M, Zannou EA, Vasanthavada M, Dontabhaktuni A, Royce AE, Joshi YM, *et al.* Measurement of Surface pH of pharmaceutical Solids: a critical evaluation of indicator dye-sorption method and its comparison with slurry pH method. J Pharm Sci. 2008;97:1831–42.
22. Govindarajam R, Zinchuk A, Hancock B, Shalaev E, Suryanarayanan R. Ionization states in the microenvironment of solid dosage forms: effect of formulation variables and processing. Pharm Res. 2006;23 (10):2454–68.
23. Qiu Y, Chen Y, Liu L, Zhang G. Developing solid oral dosage forms: pharmaceutical theory and practice. p130.
24. Li Y, Sanzgiri YD, Chen Y. A study on moisture isotherms of formulations: the use of polynomial equations to predict the moisture isotherms of tablet products AAPS Pharm Sci Tech; 2003 4(4) Article 59.
25. Brown ME, Glass BD. Pharmaceutical applications of the Prout-Tompkins rate equation. Int J Pharm. 1999;190:129–37.
26. Zannou EA, Ji Q, Joshi YM, Serajuddin ATM. Stabilization of the maleate salt of a basic drug by adjustment of microenvironmental pH in solid dosage form. Int J Pharm. 2007;337:210–8.